

# Monolithically Integrated Gain-Flattened Ring Mode-Locked Laser for Comb-Line Generation

John S. Parker, Ashish Bhardwaj, Pietro R. A. Binetti, Yung-Jr. Hung, and  
Larry A. Coldren, *Fellow, IEEE*

**Abstract**—We demonstrate broadband comb-line generation from an integrated multiple quantum well InGaAsP/InP passively mode-locked laser (MLL) with a gain flattening filter (GFF) based on an asymmetric Mach-Zehnder interferometer. The intracavity filter flattens the nonuniform gain profile of the semiconductor material providing a more uniform net cavity gain. The GFF MLL has a  $-10$  dB comb span of 15 nm (1.88 THz), the widest spectral width yet demonstrated for an integrated QW MLL at 1.55  $\mu\text{m}$ . The measured optical linewidth at the center of the comb is 29 MHz, the  $-20$  dB RF linewidth 500 KHz, while the output spectrum is phase-locked to produce 900 fs pulses at a repetition rate of 30 GHz with 4.6 ps integrated jitter from 100 Hz to 30 MHz.

**Index Terms**—Comb-line generation, integrated optics, mode-locked lasers, optical communication, photonic integrated circuits.

## I. INTRODUCTION

INTEGRATED InGaAsP/InP mode-locked lasers (MLLs) operating at 1.55  $\mu\text{m}$  wavelength are very stable pulse sources that can be used in a variety of applications in high-speed optical communication such as optical time domain multiplexing and optical sampling. Since a single MLL generates multiple phase-locked lasing modes that coherently add up to form the short pulses, MLLs can also be used for frequency comb-line generation (i.e. a multiwavelength source [1]) in applications including offset frequency locking [2], and light detection and ranging (LIDAR).

For wavelength-division-multiplexing (WDM) applications, a broadband phase-locked comb of frequencies can be used for rejection of cross-talk to allow more closely spaced non-return-to-zero (NRZ) channels and a higher spectral density [3]. In coherent communication systems, such frequency combs can greatly reduce the required front- and back-end footprint and overhead for laser stabilization and carrier tracking [4]. For

Manuscript received July 19, 2011; revised September 22, 2011; accepted October 21, 2011. Date of publication October 28, 2011; date of current version January 5, 2012. This work was supported in part by the Defense Advanced Research Projects Agency (DARPA) Photonic Integrated for Coherent Optics (PICO) Program. A portion of this work was done at the UCSB Nanofabrication Facility, part of the National Science Foundation (NSF) funded NNIN Network.

J. S. Parker, A. Bhardwaj, P. R. A. Binetti, and L. A. Coldren are with the Department of Electrical and Computer Engineering, University of California, Santa Barbara, CA 93106 USA (e-mail: JParker@ece.ucsb.edu; Ashish.Bhardwaj@jdsu.com; pbinetti@gmail.com; coldren@ece.ucsb.edu).

Y.-J. Hung is with the Department of Electronic Engineering, National Taiwan University of Science and Technology, Taipei 106, Taiwan (e-mail: yungjrhung@gmail.com).

Color versions of one or more of the figures in this letter are available online at <http://ieeexplore.ieee.org>.

Digital Object Identifier 10.1109/LPT.2011.2174148

example, a frequency comb that spans 1 THz can provide 40 WDM channels, each having a bandwidth of 25 GHz and has a substantially smaller footprint than 40 single tone lasers. Furthermore, a single wavelength locker can provide stabilization for all of the comb's periodic frequency lines. A homodyne coherent receiver would typically require each channel to have its own local oscillator (LO) for carrier synchronization [5], [6] (e.g. 40 lasers and 40 optical phase-locked loops (OPLLs)). However, a single phase-locked comb with an OPLL can supply all necessary LOs for the incoming signals. Since all lasing lines are phase-locked and have fixed frequency spacing, this effectively locks all channels.

In a semiconductor MLL, the span of the comb is determined by the cavity dispersion and the gain competition between its various lasing modes. While the semiconductor medium can generate gain that spans over 100 nm, the gain competition arising from the nonuniform material gain as a function of wavelength limits the bandwidth of the resulting frequency comb. By applying an intracavity filter function as an inverse of the spectral shape of the material gain, the resulting gain flattening creates a more uniform spectral profile. This allows for wider combs as demonstrated with bench-top MLLs [7].

Previously, we have shown the generation of 600 fs pulses from a monolithically integrated 30 GHz MLL with an intracavity gain-flattening filter (GFF) [8]. Additionally, we have compared the frequency comb span of the GFF MLL to standard MLL designs on the same material platform and have shown an improvement  $>2\times$  [9]. In this letter, we present optical linewidth, RF linewidth, single sideband phase noise measurements, and a  $-10$  dB comb span of 15 nm (1.88 THz). This is the widest frequency comb generated from an integrated quantum well (QW) based MLL at 1.55  $\mu\text{m}$ , with a span matching state-of-the-art quantum-dot (QD) and quantum-dash MLLs [10]. Moreover, such GFFs can be used to improve the gain flatness on any material platform, including: QDs, QWs, and bulk.

## II. RING MLL FABRICATION

We have chosen ring-based mode-locked laser architecture due to its ease of integration with other components to realize highly versatile photonic integrated circuits (PICs). These rings and their couplers can be defined using low-cost and high throughput i-line photolithography, allowing ring MLLs to be placed anywhere on the PIC without the need for more complicated processing. Thus rings can overcome fabrication complexity faced by distributed Bragg reflector (DBR) and

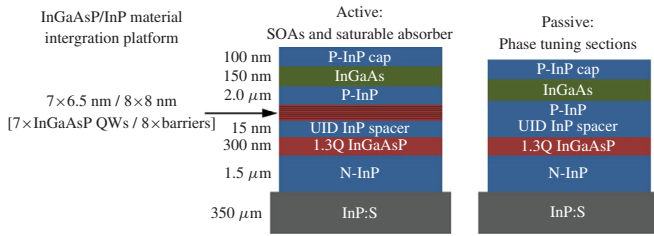


Fig. 1. Active sections (left) are used for the semiconductor optical amplifiers and the saturable absorber. The passive sections (right) are used for low-loss waveguides and phase tuning regions.

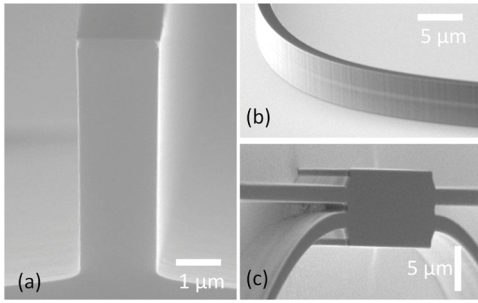


Fig. 2. Scanning electron microscope (SEM) images of the etched waveguide showing (a) 5  $\mu\text{m}$  deep etch with vertical sidewalls, (b) waveguide bends with smooth sidewalls, and (c) multimode interference (MMI) couplers.

distributed feedback lasers (DFB) that require gratings defined by holography or electron-beam-lithography, which can be expensive with reduced yield.

A ring MLL with a GFF is designed and fabricated on an InGaAsP/InP offset quantum well (OQW) platform that consists of seven 0.9% compressively strained 6.5 nm QWs and eight  $-0.2\%$  tensile strained 8 nm barriers that are epitaxially grown above a 300 nm thick 1.3Q InGaAsP layer as part of the base epi. Passive areas are defined using a selective wet-etch and a single blanket regrowth is done to cover the device with a  $\text{p}^+$ -doped InP cladding, a  $\text{p}^{++}$ -doped InGaAs contact layer, and an InP capping layer to protect the InGaAs contact layer during device fabrication. The active material is used to define the semiconductor optical amplifiers (SOAs) and the saturable absorber (SA), whereas the passive material is used to define the low-loss waveguides and current injection based phase shifters, as shown in Fig. 1.

After regrowth, the waveguide is defined with photoresist on a Cr/SiO<sub>2</sub> bilayer hard mask. The Cr is etched using a low power Cl<sub>2</sub>-based inductively coupled plasma (ICP), and the SiO<sub>2</sub> is etched using an SF<sub>6</sub>/Ar based ICP. The resulting 600 nm SiO<sub>2</sub> mask acts as a hard-mask to define the InGaAsP/InP deeply etched waveguides using a Cl<sub>2</sub>/H<sub>2</sub>/Ar (9/18/2 sccm) ICP at a chamber pressure of 1.5 mT. The resulting etched features are shown in Fig. 2. After removing the SiO<sub>2</sub> mask, blanket deposition of a 350 nm isolation layer of silicon nitride is performed. Vias are opened for top-side p-metal contacts. N-metal contacts are realized through backside deposition of Ti/Pt/Au onto the n-doped conducting InP substrate.

The fully fabricated GFF MLL PIC has a round-trip cavity length of 2600  $\mu\text{m}$ , corresponding to lasing lines spaced by

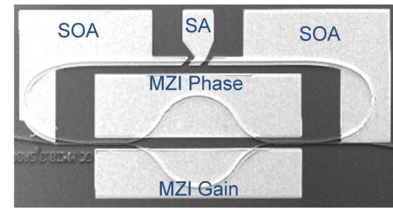


Fig. 3. SEM image of the GFF MLL PIC.

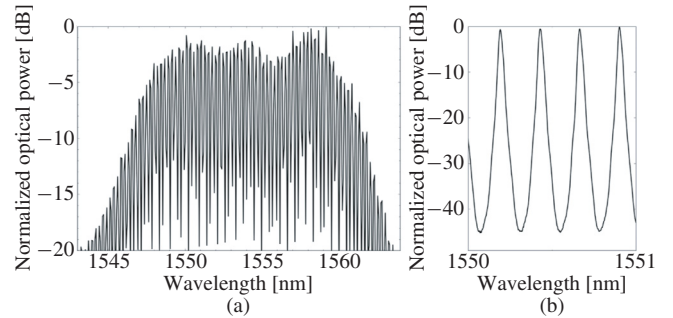


Fig. 4. Measured comb spectrum on optical spectrum analyzer (a) full span and (b) high-resolution measurement at 1550 nm showing 45 dB OSNR.

30 GHz, as shown in Fig. 3. The 600  $\mu\text{m}$  asymmetric MZI filter uses 3 dB, i.e., 50–50, multi-mode interference (MMI) couplers to form two arms, which differ in length by 16  $\mu\text{m}$  providing a free-spectral-range (FSR) of 40 nm. One of the arms of the MZI filter has an SOA that can be used to control the extinction ratio (ER) of the GFF, whereas the other arm has a phase shifter allowing adjustment of the filter zero.

### III. PHASE LOCKED COMB GENERATION

The GFF MLL PICs are mounted on copper carriers and characterized at 10  $^{\circ}\text{C}$  using a thermo-electrical cooler (TEC). For passive mode-locking, the total drive current to the two 750  $\mu\text{m}$  long ring SOAs (designated “SOA” in Fig. 3) is 110 mA with the 60  $\mu\text{m}$  long SA biased at  $-4.5$  V. The 460  $\mu\text{m}$  long MZI gain section is driven at 31 mA with the 476  $\mu\text{m}$  long MZI phase section set at 3 mA. The average power coupled into a lensed fiber is  $-6$  dBm. The MZI filter gain and phase are adjusted to maximize the optical comb width as measured on an optical spectrum analyzer (OSA), shown in Fig. 4(a). The  $-10$  dB span of the comb is 15 nm (1.88 THz) with lines spaced by 30 GHz as determined by the cavity length. As shown in Fig. 4(a), the ripple between adjacent lasing lines is several dB, while comb span is much wider. For this reason, the  $-3$  dB bandwidth often provides a poor comparison between different comb spectra, and the  $-5$  dB and  $-10$  dB bandwidths are more useful for characterization [4].

The optical signal-to-noise ratio (OSNR) over the standard 0.1 nm bandwidth is  $>35$  dB for all comb-lines, and 45 dB at the peak, as shown in Fig. 4(b).

For the temporal pulse measurements on a second-harmonic generation (SHG) based autocorrelator, the output from the GFF MLL is amplified using a 30 dBm erbium doped fiber amplifier (EDFA); this optical amplification is necessary for

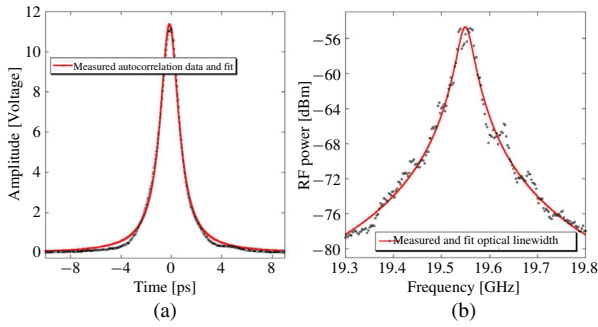


Fig. 5. (a) Measured and 900 fs Lorentzian fit pulse from an Inrad second harmonic generation based autocorrelator. (b) Heterodyne optical linewidth measurement of comb lasing line at 1555 nm. The Lorentzian linewidth fit has an FWHM of 29 MHz.

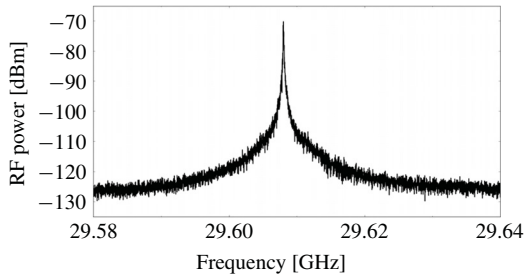


Fig. 6. Measured RF power from a 40 GHz photodiode with electrical signal analyzer (ESA). The  $-20$  dB RF linewidth is 500 KHz (RBW = 50 KHz).

measurements on the autocorrelator. Fig. 5(a) shows the narrow pulses fit to a Lorentzian function with a full width half maximum (FWHM) of 900 fs and a corresponding time bandwidth product of 1.19, 5.4x larger than the time bandwidth limit of 0.22. Added sections of single mode and dispersion compensated fiber after the EDFA did not reduce the pulse width significantly, which suggests that the EDFA introduces higher-order dispersion into the broadband pulse.

The optical linewidth at the center of the comb is measured with a heterodyne method using a 40 GHz photodiode, ESA, and a narrow  $<100$  KHz linewidth laser. Fig. 5(b) shows the Lorentzian fit optical linewidth with a FWHM of 29 MHz. The relative intensity noise (RIN) of a single mode is measured using a fiber Bragg filter centered at 1550 nm. The peak RIN is  $-82.6$  dBc/Hz at 1.18 GHz for the 110 mA drive current.

Fig. 6 shows the measured RF power from the mode-locked laser using a 40 GHz photodiode and an electrical spectrum analyzer (ESA). A 30 dB low noise microwave amplifier boosts the electrical signal in the ESA (no EDFA is used). The RF power is measured to be 50 dB above the noise floor at 50 KHz resolution bandwidth (RBW). The  $-20$  dB linewidth is as narrow as 500 KHz, demonstrating sub-MHz frequency stability between adjacent lasing lines. For use in coherent communication systems, incorporating active mode-locking into the cavity can further reduce this RF linewidth and provide precise frequency control over the mode spacing, thus enhancing the frequency stability between channels.

As shown in Fig. 7, the single sideband phase noise is measured from 100 Hz to 30 MHz with a corresponding RMS jitter value of 4.6 ps. Nearly half of the RMS jitter

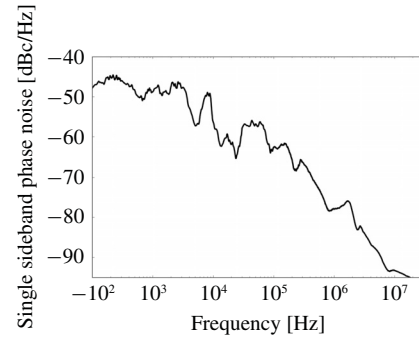


Fig. 7. Single sideband phase noise versus frequency. The integrated RMS jitter from 100 Hz to 30 MHz is 4.6 ps.

is accrued at  $<100$  KHz, which is likely due to vibrations on the optical bench and thermal instability. In practice, such low frequency noise that remains after packaging can be easily handled with receiver tracking and stabilization. We are unable to characterize the phase noise above 30 MHz, as the single sideband phase noise goes below the ESA noise floor.

#### IV. CONCLUSION

We have presented an integrated GFF MLL PIC and have demonstrated the widest integrated MLL comb span from InP-MQW based material. Changes to the cavity length can be made to accommodate frequency spacing from 10 to 40 GHz with near MHz accuracy, as determined by optical lithography. For sub-MHz frequency accuracy, active-mode locking techniques can be used. This 1.88 THz phase-locked comb source can have important applications in coherent communication systems, offset locking, and phase-locked sources for WDM.

#### REFERENCES

- [1] P. J. Delfyett, *et al.*, "Optical frequency combs from semiconductor lasers and applications in ultrawideband signal processing and communications," *J. Lightw. Technol.*, vol. 24, no. 7, pp. 2701–2719, Jul. 2006.
- [2] U. Gliese, *et al.*, "A wideband heterodyne optical phase-locked loop for generation of 3–18 GHz microwave carriers," *IEEE Photon. Technol. Lett.*, vol. 4, no. 8, pp. 936–938, Aug. 1992.
- [3] A. D. Ellis and F. C. G. Gunning, "Spectral density enhancement using coherent WDM," *IEEE Photon. Technol. Lett.*, vol. 17, no. 2, pp. 504–506, Feb. 2005.
- [4] Y. B. M'Salleem, *et al.*, "Quantum-dash mode-locked laser as a source for 56-Gb/s DQPSK modulation in WDM multicast applications," *IEEE Photon. Technol. Lett.*, vol. 23, no. 7, pp. 453–455, Apr. 1, 2011.
- [5] M. J. Fice, A. Chiuchiarelli, E. Ciaramella, and A. J. Seeds, "Homodyne coherent optical receiver using an optical injection phase-lock loop," *J. Lightw. Technol.*, vol. 29, no. 8, pp. 1152–1164, Apr. 15, 2011.
- [6] S. Ristic, A. Bhardwaj, M. J. Rodwell, L. A. Coldren, and L. A. Johansson, "An optical phase-locked loop photonic integrated circuit," *J. Lightw. Technol.*, vol. 28, no. 4, pp. 526–538, Feb. 15, 2010.
- [7] M. M. Mielke, G. A. Alphonse, and P. J. Delfyett, "Multiwavelength modelocked semiconductor lasers for photonic access network applications," *IEEE J. Sel. Areas Commun.*, vol. 25, no. 3, pp. 120–128, Apr. 2007.
- [8] J. S. Parker, A. Bhardwaj, P. R. A. Binetti, Y.-J. Hung, C. Lin, and L. A. Coldren, "Integrated 30 GHz passive ring mode-locked laser with gain flattening filter," in *Proc. IEEE Int. Semicond. Laser Conf.*, Kyoto, Japan, Sep. 2010, paper PD1, pp. 1–2.
- [9] J. S. Parker, *et al.*, "Comparison of comb-line generation from InGaAsP/InP integrated ring mode-locked lasers," in *Proc. IEEE Conf. Lasers Electro-Opt.*, Baltimore, MD, May 2011, paper CTuV6, pp. 1–2.
- [10] J. P. Tournenc, *et al.*, "Experimental investigation of the timing jitter in self-pulsating quantum-dash lasers operating at 1.55  $\mu\text{m}$ ," *Opt. Exp.*, vol. 16, no. 22, pp. 17706–17713, 2008.